DOI: 10.1002/cbic.201000527

Focused Directed Evolution of Pentaerythritol Tetranitrate Reductase by Using Automated Anaerobic Kinetic Screening of Site-Saturated Libraries

Martyn E. Hulley,[a] Helen S. Toogood,[a] Anna Fryszkowska,[b] David Mansell,[b] Gill M. Stephens,[c] John M. Gardiner,[b] and Nigel S. Scrutton*[a]

This work describes the development of an automated robotic platform for the rapid screening of enzyme variants generated from directed evolution studies of pentraerythritol tetranitrate (PETN) reductase, a target for industrial biocatalysis. By using a 96-well format, near pure enzyme was recovered and was suitable for high throughput kinetic assays; this enabled rapid screening for improved and new activities from libraries of enzyme variants. Initial characterisation of several single site-saturation libraries targeted at active site residues of PETN reductase, are described. Two mutants (T26S and W102F) were shown to have switched in substrate enantiopreference against substrates (*E*)-2-aryl-1-nitropropene and α-methyl-*trans*-cinnamaldehyde, respectively, with an increase in *ee* (62% (*R*) for W102F). In addition, the detection of mutants with weak activity against α,β-unsaturated carboxylic acid substrates showed progress in the expansion of the substrate range of PETN reductase. These methods can readily be adapted for rapid evolution of enzyme variants with other oxidoreductase enzymes.

Introduction

The use of enzymes in asymmetric synthesis has become an increasingly cost-effective and established technique to manufacture fine chemicals, pharmaceuticals and agrochemical intermediates.[1] This is due to the often unmatched efficiency, precision, stereo- and enantioselectivity of enzyme-catalysed reactions.[1–4] However, naturally occurring biocatalysts might lack some properties required for large-scale chemical production, such as high activity and selectivity for non-natural substrates.[5] To overcome the limitations in the functioning of enzymes in industrial biotransformations, directed evolution techniques in combination with high-throughput screening have been developed to improve the characteristics of enzymes in a targeted manner.[2,4]

These techniques involve the generation of libraries of mutant enzymes (single to multi-amino acid changes) by techniques such as random and site-directed mutagenesis of known key residues.[1,2,6] Such techniques can be applied to improving key characteristics of enzymes, such as substrate binding, stereo- and enantioselectivity of substrates and/or products, and even increasing the biocatalyst stability in industrial reaction conditions (e.g., high organic solvent content).[1,7] One drawback with such methods is the requirement of screening large numbers of library mutants to find improved biocatalysts, although recently developed methods of iterative saturation mutagenesis combined with structural- and functional-based residue targeting can dramatically reduce the library size.[6]

This approach was exemplified by applying it to the asymmetric reduction of activated C=C bonds; an important synthesis step as up to two stereogenic centres can be formed.[8] Recent work has demonstrated the biocatalytic potential of the Old Yellow Enzyme family (OYE; E.C. 1.6.99.1) in the reduction of activated α,β-unsaturated alkenes.[9] These FMN-containing, NAD(P)H-dependent oxidoreductases catalyse the reduction of α,β-unsaturated ketones, aldehydes, nitroalkenes, carboxylic acids and derivatives, to yield products with a variety of biotechnological and pharmaceutical applications (Scheme 1).[9,10] Members of this family include the enzymes OYE1 (brewer's yeast),[11] pentaerythritol tetranitrate reductase (PETN reductase; *Enterobacter cloacae* PB2),[12] YqjM (*Bacillus subtillis*),[13] and a recently described thermostable member TOYE (*Thermo-anaerobacter pseudethanolicus* E39).[14]

The OYE family of enzymes are classic examples of extensively characterised biocatalysts capable of reducing many industrially relevant substrates. However, family members also lack sufficient activity for formation of important industrial synthons, have low stereo- and/or enantioselectivity or can form the wrong enantiomer. Recent site-saturation mutagenesis studies of OYE1 at residue W116 generated mutants with reversed stereochemical outcomes compared to the wild type.[15]

[a] *M. E. Hulley, Dr. H. S. Toogood, Prof. N. S. Scrutton*
Faculty of Life Sciences, University of Manchester
131 Princess Street, Manchester M1 7DN (UK)
Fax: (+44) 161-306-8918
E-mail: nigel.scrutton@manchester.ac.uk

[b] *Dr. A. Fryszkowska, Dr. D. Mansell, Dr. J. M. Gardiner*
School of Chemistry, University of Manchester
131 Princess Street, Manchester M1 7DN (UK)

[c] *Prof. G. M. Stephens*
Department of Chemical and Environmental Engineering
University of Nottingham, University Park, Nottingham NG7 2RD (UK)

Supporting information for this article is available on the WWW under http://dx.doi.org/10.1002/cbic.201000527.

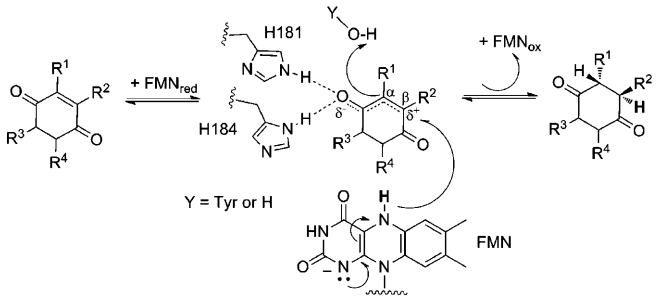

Scheme 1. General mechanism and stereochemistry of α,β-unsaturated cyclic ketone substrate reduction by PETN reductase. R^1, R^2, R^3, R^4=CH_3, H, $(CH_3)_2$, $(H)_2$ or H, CH_3, $(H)_2$, $(CH_3)_2$ for ketoisophorone bound in two conformations.

A more extensive iterative saturation mutagenesis study was conducted with the OYE homologue, YqjM, at 20 active site residue positions including C26 and Y28.[16] The screening procedures involved the use of crude cell preparations, with product detection and stereochemistry monitored by GC. A number of single and multiple residue mutants were generated with improved performance, such as enhanced steady state kinetics against selected substrates, better enantiopurity of the products, and the generation of mutants with opposite enantiopreferences.

This study describes the development of an automated, robotic anaerobic high-throughput procedure for screening libraries of enzymes against industrially useful substrates. Protocols include fully automated colony picking, extraction and microscale purification of the enzymes by using Ni-magnetic agarose beads, followed by steady state reactions with up to three substrates per library extraction. The approach taken was to screen for improvements in the steady state catalysis rather than directly monitoring for enhancement in yield and *ee*. This gives the advantages of decreased reaction times, faster screening of potential substrates, and normalisation of biocatalyst concentration. The use of purified enzymes rather than whole cell extracts allows us to remove the majority of contaminating *Escherichia coli* enzymes, such as keto reductases, which have previously been found to catalyse undesirable side reactions in the screening of YqjM mutant libraries.[16] Positive "hits" are later subjected to screening for improved yields and enantiopurity of the products. This study describes the initial high-throughput screening of libraries of single generation site-saturated mutants of PETN reductase for improvements in steady state reaction rates against a variety of typical and potential OYE substrates.

Results and Discussion

Library selection

A C-terminal His-tag was incorporated into an existing highly expressing PETN reductase construct[17,18] to enable a rapid, highly efficient and high-throughput method of biocatalyst purification. The apparent kinetic constants of both the steady state and reductive/oxidative half reactions were essentially unchanged with the substrates NADPH and 2-cyclohexen-1-one (**1 a**; Table 1; Figure S2 in the Supporting Information). This is in contrast to the OYE family member YqjM structural integrity and catalytic efficiency of which was severely compromised by the addition of a C-terminal His_6-tag.[19]

The steady-state kinetics and biocatalytic potential (yield and enantiopreference) of wild-type PETN reductase has been studied previously by using a variety of α,β-unsaturated aldehydes, ketones and nitro-olefins as substrates.[20–22] The high-throughput screening protocols were tested against libraries of single generation site-saturated mutants of PETN reductase for improvements in the steady state reaction rate of NADPH oxidation in the presence of a variety of known poor substrates, and screened against compounds not reduced by the wild-type enzyme. Mutants deemed "hits" by our protocols were produced on a larger scale (1 L) and subjected to further steady state analysis and biotransformation reactions to confirm alkene reduction had occurred, and to see whether the mutations had any effect on the product enantiopurity.

Our selection criteria for mutation positions was based on targeting residues known or predicted to be involved in substrate/inhibitor binding and/or catalysis, or due to their proximity within the active site. Previous studies have shown or predicted that residues H181, H184 and Y351 are involved in substrate/inhibitor binding in OYEs.[16,21–23] Residues W102 and T26 are positioned close to, and potentially clash or interact with picric acid and progesterone.[16,21,23,24] In addition, T26 is known to interact with the FMN cofactor and influence the redox potential of OYEs.[16,22,25] Residue Y186 was targeted; it is

Table 1. Apparent: A) steady state kinetic constants, and B) rate constants for the oxidative and reductive half reactions of PETN reductase with 2-cyclohexen-1-one **1 a**. Comparison of the apparent kinetic parameters of native and His_8-tagged PETNR.

		A) Steady state[a]			B) Half reactions[b]	
Substrate	Enzyme	k_{cat} [s^{-1}]	K_M [μM]	K_i [mM]	$k_{oxorred}$ [s^{-1}]	K_d [μM]
NADPH	wild type	8.48 ± 0.77	128.0 ± 24.5	n.d.	34.9 ± 0.4	70.9 ± 4.6
	His_8	8.72 ± 0.39	115.2 ± 11.3	n.d.	33.1 ± 0.4	81.8 ± 4.7
alkene **1 a**	wild type[c]	6.12 ± 0.17	1239 ± 81	23.3 ± 1.7	33.3 ± 1.5	8100 ± 110
	His_8	5.86 ± 0.38	1200 ± 210	21.0 ± 3.5	24.7 ± 0.8	7600 ± 810

[a] Reactions (1 mL) were performed in buffer (50 mM KH_2PO_4/K_2HPO_4, pH 7.0) containing NADPH (10–250 μM), 2-cyclohexen-1-one (**1 a**; 0.05–50 mM added as concentrated stocks in ethanol), and PETNR (100 nM). The reactions were followed continuously by monitoring NADPH oxidation at 340 nm for 2 min at 25 °C. Concentration dependence of NADPH and **1 a** was determined with a constant concentration of **1 a** (6.5 mM) and NADPH (150 μM), respectively. [b] Reactions (1 mL) were performed in buffer (50 mM KH_2PO_4/K_2HPO_4, pH 7.0) containing PETNR (100 μM) and FMN reduction/oxidation was monitored at 464 nm for 1 s at 25 °C for the reductive and oxidative half reactions, respectively. In the oxidative half reaction, PETNR FMN was previously reduced to the hydroquinone species by dithionite titration. [c] Previously published data;[20] n.d.: not determined.

the proton donor in a number of OYEs, although the role of this residue is less clear in PETN reductase.[26] Two other residues (Y68 and Q241) were targeted due to their close proximity within the substrate binding site, the latter of which is located in a highly flexible loop. We generated eight single site-saturated libraries of mutants (T26X, Y68X, W102X, H181X, H184X, Y186X, Q241X and Y351X) by PCR with degenerate oligonucleotides (NNK) at the required amino acid positions. To ensure 95% coverage of all possible amino acids per mutation site, a minimum of 94 colonies needed to be screened when using NNK degeneracy.[16] One library of 96 clones was screened per amino acid position against up to eight alkene substrates (total screening effort: 4896 individual activity rates, excluding repeats and wild-type controls).

Robotic screening optimisation and validation

To maximise the chance of detecting mutants with improved activity over wild-type enzyme, several aspects of the robotic protocols were optimised and the accuracy and reproducibility tested. Firstly, all screening procedures, excluding culture growth and centrifugation, were carried out under anaerobic conditions (< 5 ppm oxygen) to avoid significant false positive enzyme activity detection (NADPH oxidation in the absence of alkene reduction) due to unproductive flavin reoxidation by oxygen.[20] This combined with the relatively long reaction times (10 min) dramatically decreased the background levels of activity and enabled slow activities against poor substrates to be detected (results not shown). It also enabled us to screen each purified library of mutants with up to three potential substrates, which considerably reduced the costs and overall screening time.

To investigate the randomness of the mutagenesis, ten clones from each library were fully sequenced (Table S1 in the Supporting Information). Some libraries had higher randomisation rates of amino acid codons than others, and occasional additional mutations were seen (insertions and deletions), which were presumably caused by PCR error. The least randomised library was found to be Q241X, which also showed the highest frequency of premature stop codons. A more extensive sequencing of libraries H181X and H184X was conducted, with 80 and 64% of each library sequenced, respectively. Only 14 of the expected 21 outcomes (including wild type and stop codon) were detected in library H181X, with H181I being the most frequently observed mutation. In contrast, library H184X was more highly randomised and showed 20 of the expected 21 outcomes, with fewer additional mutations and a more even distribution of the mutations (results not shown).

A potential problem in comparing mutant activity data from high-throughput screening methods is the frequent variability in expression levels of mutants and consequential differences in enzyme concentrations within the assays. To avoid the necessity of determining the protein concentration of each preparation, the robotic procedures included microscale protein purification to normalise eluted enzyme concentration for the subsequent assays. To test the consistency of the eluted protein concentrations, both the expression and robotically purified protein levels of ten randomly selected clones were monitored by SDS-PAGE (Figure 1 A and B; Table S2 in the Supporting Information) and the protein concentration of the eluates was determined (Table S3 in the Supporting Information).

In all libraries (Figure 1 A and B for Y68X), variable protein expression levels were seen in whole cell extracts, yet after robotic protein microscale purification remarkably similar levels

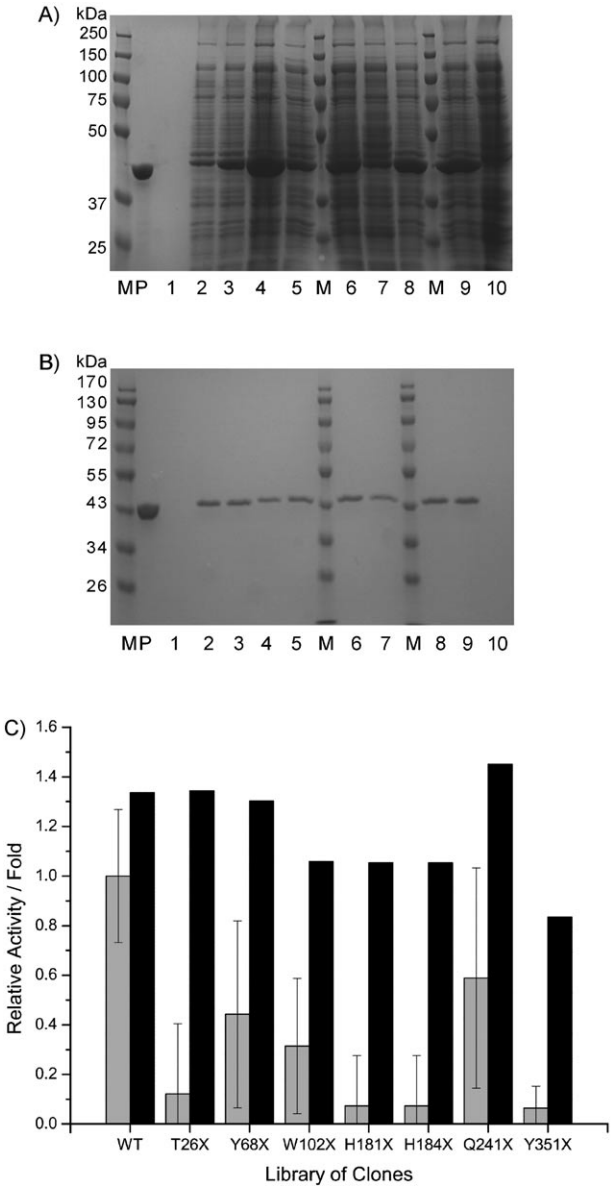

Figure 1. SDS-PAGE analysis of ten randomly selected: A) cell lysates, and B) robotically purified PETN reductase Y68X mutants. M: protein molecular mass markers; P: purified PETN reductase standard; 1: Y68V; 2: Y68N; 3: Y68G; 4: Y68L; 5: Y68K; 6: Y68R; 7: Y68Q; 8: Y68V; 9: Y68H; 10: Y68STOP. C) Average (grey bars) and maximal (black bars) relative steady state activity of each library of mutants compared to the average activity of wild-type PETN reductase (96 clones per library). The error bars denote one standard deviation of the data. Reactions (0.3 mL) were performed in buffer (50 mM KH_2PO_4/K_2HPO_4, pH 7.0) containing NADPH (100 μM) and alkene **1a** (1 mM added as a stock in ethanol), and started by the addition of PETNR eluant (50–150 μL). The reactions were continuously monitored at 340 nm for 10 min at 25 °C.

of purified protein were produced (average of (126 ± 16) μg mL^{-1} across four libraries). Some libraries showed higher variability in expression levels than others (83–100% expression of library members sampled), with the mutant clones Y186X showing such consistently poor PETN reductase expression (10% clones expressed) that further screening was abandoned.

Screening hits

Two methods were employed for defining potential "hits" in our screening protocols. Firstly, individual mutant library member activity screening data were compared to the average activity of 96 control wild-type clones that had been subjected to identical robotic procedures as the mutants (Table 2 and Table S4 in the Supporting Information; column 4). This enabled us to directly compare the reaction rates of individual mutants to wild-type activity. Due to the limitations in the number of mutants screened per library, hits were conservatively selected based on whether the activity was greater than the mean activity plus one standard deviation of the wild-type library (e.g., Figure 1C). In addition the *Z* scores of each mutant were determined; this is a reflection of the variation of individual mutant activity data against the average rate for the 96 mutants.[27] Potential hits were defined as having screening rates with a *Z* score of at least two (Table 2 and Table S4 in the Supporting Information; column 3).

As additional controls, the mutant libraries were screened with the oxidative substrates α,β-unsaturated ketone **1a** and aldehyde **3a**[20] to see whether the mutants had compromised PETN reductase-like activity. All the mutants tested against alkene **1a** had lower specific activities than the wild type (Table 2). Most of the hits with substrate **3a** had essentially the same specific activity as wild-type enzyme including T26S and Q241L. Interestingly, mutation H184N gave PETN reductase the highly conserved OYE-like active site substrate binding pair H181/N184, yet showed only 15% activity with alkene **1a** (Table 2); this highlights the importance of the His/His couple in this enzyme. On the whole, libraries Q241X and Y68X retained relatively good levels of activity compared to wild-type enzyme, while libraries H181X, H184X and Y351X showed typically very poor activity. As our assay method detects levels of NADPH oxidation, it is not clear whether the changes in the reactions rates with the mutation is at least partly due to changes in its reactivity with and/or binding to NADPH.

The most dramatic increases in activity were seen with the W102X library against alkenes **2a** and **4a**. Mutants W102F and W102I showed five- and sixfold increases in steady state rate, respectively, against the relatively poor substrate 2-methylcyclopenten-1-one (**2a**). More moderate increases in activity (about twofold) were seen with the mutations T26A and Q241W. This is in comparison to mutagenesis studies of the OYE morphinone reductase that showed mutant T32A (equivalent to PETN reductase T26A) had a reduction in redox potential of FMN by ~50 mV, and changes in both the catalytic rate (k_{cat}) and binding (K_M) of both the reductive and oxidative substrates.[25]

Table 2. Relative screening rates and steady state kinetics of PETN reductase mutants with ketone-, aldehyde- and acid-containing alkenes.

Substrate	Mutant	Potential hits[a] (*Z* score)	Relative rate[b] (fold)	Rate[c] [s^{-1}]
 **1a**	wild type	–	1.0	3.25 ± 1.05
	T26S	3.8 (3.0)	1.2	0.55 ± 0.11
	Y68L	2.2 (1.7)	1.3	0.80 ± 0.07
	W102Y	2.5 (1.5)	1.0	0.55 ± 0.09
	H184N	1.1 (4.2)	0.2	0.50 ± 0.12
	Q241T	1.9	1.4	1.56 ± 0.63
	Y351F	0.8 (3.9)	0.1	0.79 ± 0.02
 **2a**	wild type	–	1.0	0.11 ± 0.01
	T26A	2.9 (2.5)	0.8	0.20 ± 0.01
	Y68F	4.0 (1.4)	1.4	0.28 ± 0.00
	W102F	3.2 (0)	2.7	0.54 ± 0.01
	W102I	3.3 (0)	2.4	0.66 ± 0.03
	Q241V	2.6	0.9	0.20 ± 0.01
	Q241W	2.7	0.9	0.21 ± 0.04
	Y351M	2.6 (1.3)	0.6	0.11 ± 0.01
	Y351P	2.4 (1.3)	0.6	0.15 ± 0.01
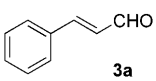 **3a**	wild type	–	1.0	1.86 ± 0.14
	T26S	2.8 (4.0)	0.9	1.98 ± 0.10
	Y68S	1.9 (2.4)	1.0	0.92 ± 0.02
	Q241L	2.0	1.5	2.17 ± 0.07
	Q241V	1.6	1.3	2.15 ± 0.06
	Y351F	0.6 (5.3)	0.1	0.23 ± 0.02
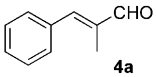 **4a**	wild type	–	1.0	0.43 ± 0.00
	T26A	0.9 (3.6)	0.3	0.14 ± 0.01
	Y68S	2.7 (1.1)	2.3	0.07 ± 0.00
	W102F	2.1 (0.5)	2.7	3.91 ± 0.15
	W102Q	2.0 (0.5)	2.6	1.25 ± 0.04
	Q241L	2.0	2.2	0.54 ± 0.01
	Q241V	1.6	2.0	0.27 ± 0.00
	Y351F	0.7 (4.7)	0.1	0.12 ± 0.00
 **5a**	wild type	–	1.0	0.01 ± 0.00
	T26A	1.7 (0.2)	5.4	0.02 ± 0.00
 **6a**	wild type	–	n.a.	n.d.
	H184F	2.5 (2.5)	n.a.	0.01 ± 0.00
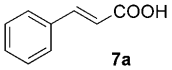 **7a**	wild type	–	n.a.	n.d.
	H181I	2.9	n.a.	0.01 ± 0.00
	H181S	4.2	n.a.	0.01 ± 0.00

[a] Values in parentheses are the average *Z* score from confirmed wild-type members within each library. No confirmed wild-type PETN reductase clones were found in the Q241X library. [b] Reactions (0.3 mL) were performed in buffer (50 mM KH_2PO_4/K_2HPO_4, pH 7.0) containing NADPH (100 μM) and alkene (1 mM added as concentrated stocks in ethanol), and started by the addition of robotically purified PETNR eluant (50–150 μL). The reactions were followed continuously by monitoring NADPH oxidation at 340 nm (365 nm for **4a**) for 10 min at 25 °C. Relative rates are expressed as the ratio of activity of each mutant relative to the mean activity of 96 wild-type control clones in a separate library. [c] Steady state kinetics of wild-type and mutant PETN reductases generated by using conventional purification techniques. Reactions (0.3 mL) were performed as above except for the PETN reductase concentration (50–2000 nM) and reaction time (2 min); n.a.: not applicable; n.d.: no activity detected.

Mutations W102Q and W102F showed 2.8- to ninefold increase in rate against substrate **4a**, while two other mutants showed essentially the same rate as wild type (Q241L and Q241V). Interestingly, enzymes W102F/I are equivalent to improved mutants of OYE1 W116F/I, which showed a reversal in stereochemistry against the substrate (*S*)-carvone due to the substrate binding in a "flipped" orientation.[15] Similarly, a screen of the equivalent residue in YqjM generated four single mutants (A104F/W/H/Y) with altered conversion rates and/or enantioselectivity.[17] PETN reductase residue W102 has previously been identified as potentially influencing the binding of larger substrates and inhibitors.[16,21,23,24] The substitution for smaller hydrophobic residues, such as phenylalanine and isoleucine, might influence the degree of orientation of substrate binding without significantly altering the localised hydrophobic environment.

Few confirmed hits were obtained when screening against poor or nonsubstrates of PETN reductase, such as 3-methyl-cyclohexen-1-one (**5a**), and α,β-unsaturated carboxylic acids **6a**–**7a** yielded few confirmed hits (Table 2). Activity was improved against alkene **5a** to a moderate extent with the mutation T26A, while weak activity was detected with carboxylic acid-containing substrates **6a**–**7a**, which were not reduced by wild-type PETN reductase, with mutants H184F and H181I/H181S, respectively. Libraries screened against other substrates (3-methyl-cyclopenten-1-one (**8a**), cinnamonitrile (**9a**), cyclohexene carbonitrile (**10a**), and methyl cinnamate (**11a**); Table S4 in the Supporting Information) yielded no confirmed hits. Some false positive hits with substrates **8a** and **11a** in the Q241X library included changes to Asp, Val and His (Table S4 in the Supporting Information). Overall, out of 56 possible hits, there were six confirmed minor improvements in catalytic activity (>twofold; five mutations), three of which came from the W102X library (Table S4 in the Supporting Information).

Biotransformations with confirmed mutants

A number of mutants had been identified as potentially useful by kinetic screening, however, these assays monitor NADPH oxidation, and so, are an indirect measure of alkene reduction. To see what impact these mutations had on alkane product yields and/or enantiopurity, biotransformation reactions with the mutants were performed. Wild-type PETN reductase has been shown previously to reduce α-methylcinnamaldehyde (**4a**) with reasonable conversions, but poor *ee* values,[28] in agreement with our results (5–13% *ee*; 99–100% yield; Table 3). To our surprise, mutant W102F reduced alkene **4a** with a significant increase in product *ee* (62% vs. 13%) and a switch in product enantiopreference to the *R* enantiomer. In addition, mutant Y351F showed a moderate increase in enantiopurity of (*S*)-**4b**. In all reactions with alkene **4a**, the product *ee* was significantly higher after 4 h than after 24 h reactions, probably due to product racemisation in aqueous media as seen with α,β-disubstituted nitroalkanes.[20,22,29]

A switch in product enantiopreference caused by a single amino acid change is remarkable, but not unique. Mutations of the equivalent residue W116 of OYE1 to phenylalanine resulted in the formation of (*R*)-citronellal from neral compared to the (*S*)-enantiomeric product with wild-type enzyme.[15] In addition, there was an increase in *ee* from 19 to 65%, similar to our results with W102F reduction of **4a**. The OYE1 mutant W116I showed a switch in product enantiopreference in reactions with (4*S*)-carvone, with a dramatic increase in *ee*. Previous studies with YqjM showed that mutation of the equivalent residue A104 to phenylalanine did not show a switch in product enantiopreference, but did result in a small increase in conversion and *ee*.[16]

The co-crystal structures of wild-type PETN reductase and mutants W102F and W102Y complexed with picric acid were determined previously.[30] A comparison of the structures showed no major structural changes, however, the conversion of W102 to phenylalanine removed the hydrogen bond between W102 NE1 and Q60 NE2 present in the wild-type structure.[24] Solution studies indicated that picric acid was bound more tightly to the active site of the two mutant enzymes, with no significant impairment of FMN reduction by NADPH. This was further supported by the co-crystal structures, which showed both a higher occupancy of bound picric acid and a shift in position of binding to the mutant enzymes due to the removal of clashes with W102 atoms CZ3 and CH2.[30] Taken together, these results suggest that residue W102 plays a critical role in the orientation of the substrate in the active site. Mutations at this position could impact on the relative occupancy of the substrate in the different binding conformations, which in turn might affect the stereochemistry of the product and the overall catalytic rate.

When PETN reductase library Q241X was screened against cinnamaldehyde derivatives **3a**–**4a**, a hit was obtained with mutant Q241L with both substrates (Table 3). Surprisingly, this mutant showed similar conversions and *ee* values to the wild type, but the yield of product **4b** was dramatically reduced. This was due to the reduction of the aldehyde to form significant quantities of the equivalent phenylethanol derivatives as side products. Similarly, reductions of **4a** with the mutant W102Q yielded almost entirely 2-phenyl-propan-1-ol, while wild-type and other mutant reactions generated only small quantities of side products (up to 6%). While PETN reductase enzyme preparations were typically ~95% pure, some minor contaminants were seen in SDS-PAGE analysis of the Q241L mutant. The contaminating proteins were analysed by in-gel trypsin digestion followed by mass spectrometry,[31] and revealed the presence of an *E. coli* putative zinc-type alcohol dehydrogenase-like protein, YahK, similar to biotransformations with extracts of YqjM mutants[16] (results not shown). It is presumed that such contaminating enzymes can be responsible for the aldehyde to alcohol conversion. The absence or low quantities of alcohol by-products in reactions with other mutants against aldehyde substrates suggest that protein purification had been more successful in removing the contaminating alcohol dehydrogenase activity.

Reactions of PETN reductase mutants T26A and Y68F with the cyclopentenone substrate **2a** showed a reduction in conversion and yield by about a third compared to the wild-type enzyme. This compares to reactions with mutant W102F, which

Table 3. Reduction of activated alkenes by PETNR wild-type and library mutants using NADPH.[a]

Substrate	Product	Enzyme[b]	Conv.[c] [%]	Yield[c] [%]	By-product(s)[d] [%]	*ee*[d] [%]
 **1a**	 **1b**	wild type	100 (100)	93 (100)	0	n.a.
		T26S	100 (100)	100 (96)	0	n.a.
		Y68L	100 (100)	100 (82)	0	n.a.
		W102Y	100 (100)	100 (90)	0	n.a.
		Q241T	100 (100)	100 (88)	0	n.a.
		Y351F	100 (100)	100 (85)	0	n.a.
 **2a**	 (*S*)-**2b**	wild type	89	89	0	69
		T26A	59	59	0	56
		Y68F	59	53	0	49
		W102I	93	82	0	72
		W102F	93	81	0	46
		Q241V	72	72	0	62
		Q241W	89	89	0	66
		Y351M	84	84	0	66
		Y351P	94	94	0	70
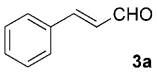 **3a**	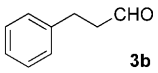 **3b**	wild type	93 (72)	93 (72)	0 (<1)	n.a.
		T26S	100 (82)	100 (69)	0 (<1)	n.a.
		Y68S	92 (92)	91 (68)	0 (<1)	n.a.
		Q241L	100	57	43	n.a.
		Y351F	95 (100)	95 (32)	0 (<1)	n.a.
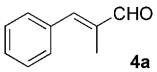 **4a**	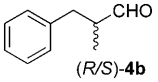 (*R/S*)-**4b**	wild type	100 (99)	100 (99)	2 (<1)	5 (13) (*S*)
		T26A	100 (10)	98 (0)	6 (0)	7 (0) (*S*)
		Y68S	99 (81)	90 (77)	8 (6)	1 (6) (*R*)
		W102F	99 (100)	94 (97)	5 (3)	18 (62) (*R*)
		W102Q	100	1	99	n.d.
		Q241L	99	77	22	3 (5) (*S*)
		Y351F	99 (99)	94 (99)	2 (1)	14 (38) (*S*)
 **5a**	 (*S*)-**5b**	wild type	29	29	0	98
		T26A	52	52	0	66
		Y68L	8	8	0	n.d.
		W102D	0	0	0	n.d.
		W102I	0	0	0	n.d.
		Q241W	10	10	0	91
		Y351E	8	8	0	n.d.
 **8a**	 (*S*)-**8b**	wild type	9	9	0	>99
		T26L	1	0	0	n.d.
		W102Y	1	1	0	n.d.
		H181D	0	0	0	n.d.
		H181Y	0	0	0	n.d.
		Q241D	1	1	0	n.d.
		Q241V	4	4	0	n.d.
		Y351M	11	11	0	>99

[a] Conditions: standard reactions (1.0 mL) were performed in buffer (50 mM KH_2PO_4/K_2HPO_4, pH 7.0) containing alkene (5 mM; added as a concentrated stock in ethanol), NADPH (6 mM) and PETN reductase (2 μM). The reactions were shaken at 37 °C at 130 rpm for 4 or 24 h. Reactions in parentheses were performed for 4 h. [b] Wild-type data were determined previously.[20,22] [c] Determined by GC by using DB-Wax column. [d] Determined by GC or HPLC; n.a.: not applicable; n.d.: not determined.

showed similar product yields as wild type, but a significant drop in *ee*. Biotransformations of almost all mutants tested with the related poor substrate 3-methyl cyclopenten-2-one (**8a**) showed essentially no activity compared to an 8% yield for the wild-type enzyme. The only mutant with significant activity was Y351M, which yielded 11% product with >99% *ee*.

Mutations at equivalent residues in YqjM and/or OYE1 gave similar types of changes to those observed for PETN reductase

mutants. YqjM mutants C26A and A102F (equivalent to T26A and W102F in PETN reductase) gave slightly lower %*ee* values and minor changes in conversion rates compared to wild-type enzyme with related substrates cyclohex-2-en-1-one-3-methyl carboxylate and cyclopent-2-en-1-one-3-methyl carboxylate.[16] However, the YqjM mutant A102W, which is equivalent to wild-type PETN reductase, showed no significant change in conversions and %*ee* to wild-type enzyme.

Mutant Y351F reduced substrates **1a** and **3a** with a dramatic decrease in product yield after 4 h, but not 24 h compared to wild-type enzyme. These results are consistent with the observed differences in steady state reaction rates with these mutants (Table 3). This is an example of how mutations causing moderate decreases in steady state rates can still be useful biocatalysts as the reduction in rate can be compensated for by running biotransformations for extended time periods (24 h vs. 2 min). Interestingly, in some cases specific mutations would only show significant changes in reactions against some of the substrates tested. For example, mutants W102I and Q241W showed dramatic decreases in conversion with substrate **5a**, but not **2a**. This highlights the importance of screening libraries of mutants against multiple substrates as specific mutations are unlikely to improve the PETN reductase-catalysed reduction of all target alkenes.

Biotransformations of PETN reductase T26S mutant

Although the mutant T26S did not show significant improvements in the screening reactions, it was selected for further investigation as previous studies with the wild-type enzyme suggested the loss of the side chain methyl group (CG2 of T26) might potentially remove clashes with some substrates.[15,20,21,23] In addition, the mutant is likely to retain both hydrogen bonds between residue 26 and the FMN seen in the wild-type structures[23] due to the retention of the OG atom in S26. Therefore, reactions with wild type and T26S mutant were carried out with 2- or 3-methyl substituted cyclopenten-1-one and cyclohexen-1-one derivatives **2a**, **5a**, **8a** and **12a**, aldehydes **13a**–**15a**, (*R*)-carvone ((5*R*)-**16a**), ketoisophorone (**17a**), *N*-phenylmethyl maleimide (**18a**), and nitro-olefins (*E*)-**19a** to (*E*)-**22a** over 24 h by using NADPH and/or a $NADP^+$/G6PDH cofactor regenerating system (Table 4). In spite of a near sixfold reduction in steady state rate of T26S with alkene **1a** compared to wild-type enzyme (Table 2), this did not significantly effect the yield and enantioselectivity when biotransformations were performed for 24 h.

The reactions with the cyclic ketone substrates **12a** and **17a**–**18a** with the wild type and T26S generated the *R* products with high yields and enantiopurities, while reactions with substrates **5a**–**6a** and **15a** yielded only low levels of highly enantiopure products. In contrast, the reaction of T26S with 2-methylcyclopent-2-en-1-one (**2a**) showed a considerable decrease in conversion and yield compared to wild-type enzyme, although similar product enantiopurities were seen. Both the wild-type enzyme and T26S mutant generated high yields of the (*rac*)-**20b** product, which should be attributed to product racemisation rather than a lack of enzyme stereoselectivity.[20]

The most dramatic change was seen in reactions of T26S with the nitro-olefin substrate (*E*)-**19a**. The mutant preferentially catalysed the formation of *R* enantiomer of product **19b** (37–44% *ee*) whereas the wild-type enzyme yielded the *S* enantiomer (48–37% *ee*). Moreover, less by-product formation—namely the corresponding oxime—was observed for this mutant (Table 4). Interestingly, the switch of enantiopreference was not observed for the equivalent *p*-chlorinated substrate (*E*)-**21a**, which was reduced to (*S*)-**21b** by both enzymes. PETN reductase is known to reduce the *E* isomers of 2-aryl-1-nitropropenes with variable enantioselectivity due to a nonenzymatic *E*/*Z* isomerisation of the substrates,[26] in addition to other factors, such as the nature of the cofactor.[9]

In addition, the poor *ee* values are thought to be due to the possibility of multiple binding conformations of the *E* isomers of the substrates in PETN reductase (Scheme 2). The removal of the CG2 methyl group of T26 appears to have altered the shape of the substrate binding site to enable an increase in the binding of the substrate in the "flipped" binding mode,[22,23] thereby, improving the yield of the (*R*)-**19b** product. Interestingly, the reaction of T26S with the *p*-chlorinated substrate (*E*)-**21a** resulted in a significant increase in *ee* compared to wild type; this also suggests a change in the relative active site occupancy of the substrate in the different binding conformations.

Previous kinetic studies of the wild-type enzyme showed that the reduction of (*Z*)-**19a** is rapid and quantitative, and yields almost enantiopure products.[26] This contrasts with the reduction of (*E*)-**19a**, which is considerably slower (~30-fold) with poorer product enantiopurities. These results suggest that (*Z*)-**19a** binds more optimally compared to (*E*)-**19a**, with the possibility of multiple binding conformations with (*E*)-**19a**. A model of the preferred substrate (*Z*)-**1a** bound to wild-type PETN reductase shows both the nitro group and the phenyl ring pointing down towards the ribityl chain of FMN, to yield (*S*)-**19b** (Scheme 2A). In this position, the nitro group interacts with H181 and/or H184. In contrast, (*E*)-**19a** would need to bind in the "flipped" binding conformation to produce the (*S*)-**19b** product. To produce (*R*)-**19b**, the substrate (*E*)-**19a** would need to bind in a more conventional conformation, as seen for (*Z*)-**19a** binding, with the nitro group pointing downwards (Scheme 2B). Such binding conformations could reduce any potential clash between the substrate methyl substituent and T26 CG2 atom. This could explain why (*S*)-**19b** is the preferred enantiomeric product of (*E*)-**19a**, as the binding mode to produce (*R*)-**19b** is likely to cause a clash between the substrate phenyl ring and T26 CG2 atom (Scheme 2B).

Nitroalkene (*E*)-**19a** has been shown to undergo a slow, reversible isomerisation to (*Z*)-**19a** under the reaction conditions (Scheme 2C).[20] This suggests that the moderate enantiopurities of alkane **19b** obtained during the reduction of (*E*)-**19a** with both wild-type and T26S PETN reductase might be at least partially due to a form of dynamic kinetic resolution.[29] In this case, the binding of (*E*)-**19a** in a (*Z*)-**19a**-like manner would lead to a slow reduction (k_i) to (*R*)-**19b**, while (*Z*)-**19a** formed by isomerisation is likely to bind to PETN reductase in the conventional manner to rapidly form (*S*)-**19b** (~30 k_i;

Table 4. Reduction of various activated alkenes by PETNR wild-type and T26S mutant by using $NADP^+$/G6PDH cofactor regeneration system or NADPH.[a]

Substrate	Product	Enzyme[b]	*t* [h]	Conv.[c] [%]	Yield[c] [%]	*ee*[d] [%]
 **2a**	 (*S*)-**2b**	wt-NADPH	48	>99	99	57
		wild type	24	62	62	70
		T26S	24	23	16	69
 **5a**	 (*S*)-**5b**	wt-NADPH	48	39	37	>99
		wild type	24	25	18	>99
		T26S	24	28	13	>99
 **8a**	 (*S*)-**8b**	wt-NADPH	48	23	22	>99
		wild type	24	14	14	>99
		T26S	24	9	7	>99
 **12a**	 (*R*)-**12b**	wt-NADPH	48	>99	95	95
		wild type	24	>99	93	97
		T26S	24	92	80	96
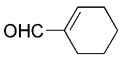 **13a**	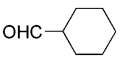 **13b**	wt-NADPH	48	>99	78	n.a.
		wild type	24	>99	85	n.a.
		T26S	24	>99	84	n.a.
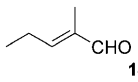 **14a**	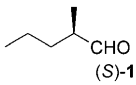 (*S*)-**14b**	wt-NADPH	48	>99	78	27
		wild type	24	>99	85	66
		T26S	24	>99	84	70
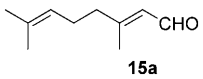 **15a**	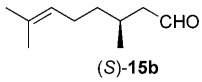 (*S*)-**15b**	wt-NADPH	48	>99	18	>95
		wild type	24	>99	23	>95
		T26S	24	>99	33	>95
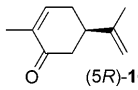 (5*R*)-**16a**	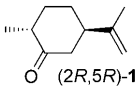 (2*R*,5*R*)-**16b**	wt-NADPH	24	>99	88	93 *de*
		wild type	24	>99	76	94 *de*
		T26S	24	>99	95	94 *de*
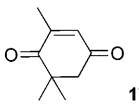 **17a**	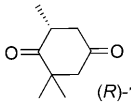 (*R*)-**17b**	wild type	1.5	>99	80	95
		T26S	1.5	>99	89	95
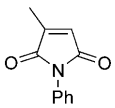 **18a**	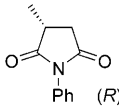 (*R*)-**18b**	wild type	48	>99	>99	>99
		T26S	48	>99	>99	>99
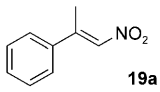 **19a**	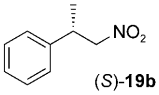 (*S*)-**19b**	wild type	48 (48)	90 (>99)	72[e] (88)	48 (37)
		T26S	48 (48)	>99 (>99)	37[e] (>95)	37 (44) (*R*)
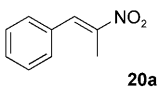 **20a**	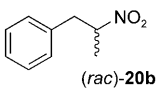 (*rac*)-**20b**	wild type	48	>99	93	0
		T26S	48	>99	92	0
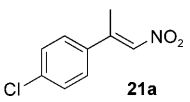 **21a**	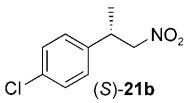 (*S*)-**21b**	wild type	48 (48)	78 (77)	63[e] (50)	67 (55)
		T26S	48 (48)	65 (58)	55[e] (44)	82 (87)

Table 4. (Continued)

Substrate	Product	Enzyme[b]	*t* [h]	Conv.[c] [%]	Yield[c] [%]	*ee*[d] [%]
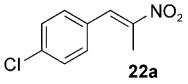 **22a**	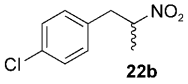 **22b**	wild type	7 d	64	40	64
		T26S[f]	7 d	60	38	60
		wild type	48	92	88	20
		T26S	48	84	84	13
		wild type[f]	7 d	>99	97	73
		T26S[f]	7 d	86	86	60

[a] Conditions: reactions (1 mL) were performed in buffer (50 mM KH_2PO_4/K_2HPO4, pH 7.0), alkene (5 mM; added as a DMF solution with 2% (*v/v*) final concentration), PETNR (2 μM), glucose-6-phosphate dehydrogenase (8 U), glucose-6-phosphate (20 mM) and $NADP^+$ (6 μM). Reactions were agitated at 30 °C at 130 rpm. Values in parentheses were repeated reactions. [b] Wild-type data were determined previously.[20,22] [c] Determined by GC by using DB-Wax column. [d] Determined by GC or HPLC. [e] Oxime by-product detected. [f] Biphasic reactions: reactions were carried out anaerobically in 30 mL screw top vials sealed with PTFE-silicon septa. Each reaction mixture (12 mL) contained buffer (50 mM KH_2PO_4/K_2HPO_4, pH 7.0) containing nitroalkene (1.7 mM) dissolved in 4.8 mL anaerobic *iso*-octane, PETN reductase (~3 μM), NADP (20 μM) glucose-6-phosphate (14–20 mM), glucose-6-phosphate dehydrogenase (10 U) and *sec*-butyl benzene (25 μL). Reactions were agitated at 200 rpm for 1–7 days at 30 °C. [g] Absolute configuration uncertain; n.a.: not applicable; d: days. wt-NADPH: wild-type PETN reductase reactions performed in the presence of NADPH.

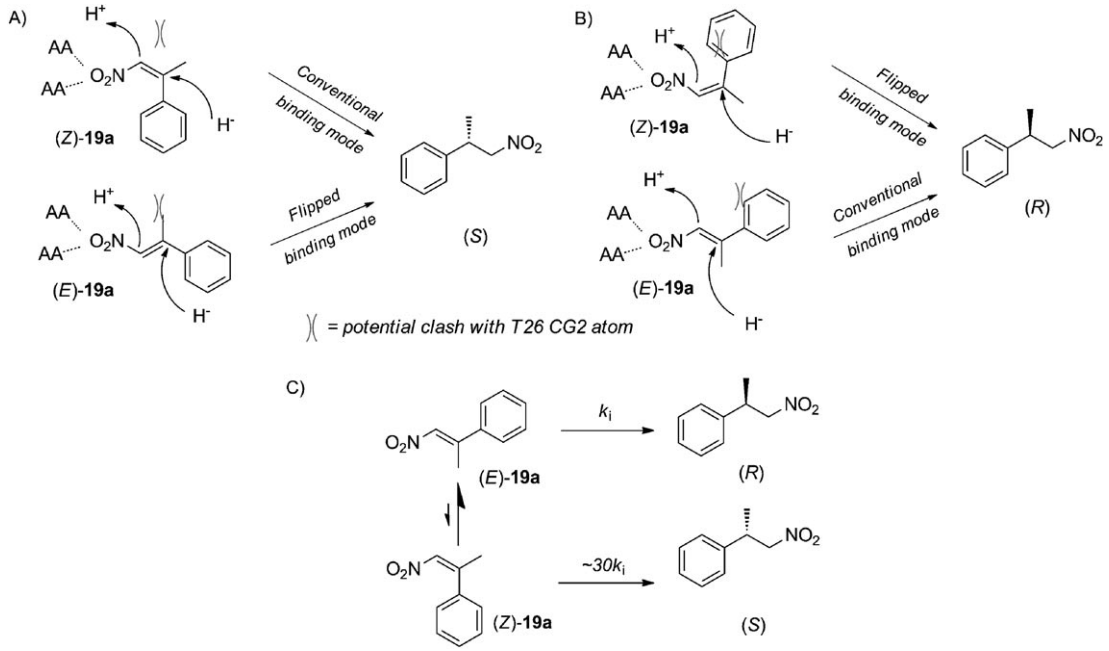

Scheme 2. Predicted binding modes of the PETN reductase-catalysed reduction of the nitro-olefin substrate (*Z*)- and (*E*)-**19a** to form: A) (*S*)-**19b**, and B) (*R*)-**19b**. C) Model of the proposed dynamic kinetic resolution of (*E*)-**19a** by a combination of (*E*)- to (*Z*)-**19a** isomerisation combined with both forms of the substrate binding to the enzyme in the conventional manner.

Scheme 2C). The switch in product stereochemistry by the T26S mutant is suggestive of an increase in the relative population of the *E* substrate in the conventional binding conformation, which is likely due to the removal of a potential clash between the substrate phenyl ring and the T26 CG2 atom. Several studies[9,20] have demonstrated variability in enantiopurity and stereochemistry of OYE-catalysed reductions depending on factors such as the cofactor used and reaction time, which could impact on substrate binding, enzyme kinetics and substrate isomerisation. Therefore, in the absence of a co-crystal structure of (*E*)- or (*Z*)-**19a**-bound PETN reductase, the exact cause(s) of the moderate product *ee* values are not known.

In addition to the changes seen in product *ee* and/or enantioselectivity, reactions with (*E*)-**19a** and (*E*)-**21a** with both the wild-type and T26S enzyme gave lower than expected product yields. This was due to the formation of significant quantities of the equivalent oxime, aldehyde, alcohol and other unidentified by-products, as seen previously with wild-type PETN reductase (Scheme 3).[26] Oxime formation from aliphatic and aromatic nitro compounds has also been seen with other OYEs.[32] The mechanism of OYE-catalysed oxime formation is not clear; however, others have suggested that it proceeds after alkane product formation by the reduction of the nitro group to yield the nitroso derivative, which spontaneously rearranges to form

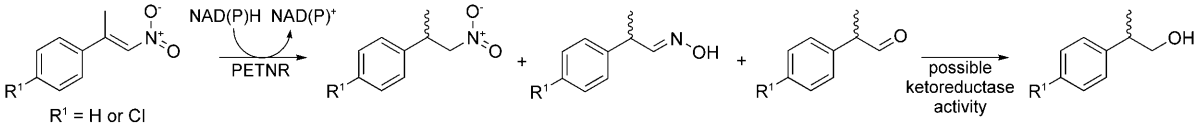

Scheme 3. Products obtained from the reactions of nitro-olefins (*E*)-**19a** and (*E*)-**21a** with wild-type and T26S mutant PETN reductase. Further unidentified minor side products were also produced. The formation of the alcohol product might be due to the reduction of the equivalent aldehyde, possibly by the presence of a minor contaminating keto-reductase.

the oxime.[32] However, our studies suggest that PETN reductase-catalysed oxime formation proceeds by nitro reduction of the alkene substrate rather than the equivalent alkane product (results not shown). Further discussion and possible mechanisms of oxime formation will be presented elsewhere.

The general trend seen with reactions containing NADPH versus the $NADP^+$/G6PDH recycling system is an increase in % conversion (Table 4) due to the longer time scale of the reactions (48 vs. 24 h). However, the wild-type enzyme gave lower yields of products with aldehyde substrates **14a** and **15a** in the presence of NADPH due to an increase in the levels of side products. In addition, the enantiopurity of **14b** was dramatically reduced in the longer reactions presumably due to water-mediated racemisation of the product.[9,20,33] This was also seen in the reactions with substrate **2a**, which has previously been shown to undergo a time-dependent loss of product enantiopurity under aqueous conditions.[20]

Recent site-saturated mutagenic screening of YqjM at the equivalent residue C26 by others[16] against the non-wild-type substrate 3-ethylcyclohex-2-en-1-one yielded six mutants capable of reducing this compound. Mutants C26V/G/D were capable of forming the *S* enantiomer of product 3-methyl-2-cyclohexan-1-one with moderate enantiopurities. This is similar to reductions of the poor substrate 3-methyl-2-cyclohexen-1-one (**5a**) with PETN reductase, which yielded the *S* enantiomeric product with low yields, but high enantiopurities. This residue in OYEs, which is known to interact with the FMN via backbone and side chain interactions,[14,16,34] is thought to increase the enzyme redox potential by stabilising the negative charge of the reduced flavin.[34] The loss of the hydrogen bond between the OG1 atom of the equivalent residue T37A of OYE1 (SG atom of C26 in YqjM) decreases the redox potential of the enzyme by 33 mV; this results in both a decrease and an increase in the reductive and oxidative half reactions, respectively. It is apparent that residue T26 is a key target in fine-tuning the enantiopreference of these enzymes against a number of substrates. Interestingly, the YqjM mutants C26T or C26S (equivalent to wild-type and T26S of PETN reductase, respectively) were not apparent "hits" with this substrate.[16]

Structure of PETN reductase mutant T26S

The X-ray crystal structure of the wild-type His_8-tagged PETN reductase was determined to 1.4 Å to see if the presence of the non-native C-terminal tag had any impact on the overall structure of the enzyme. In addition, the crystal structure of the T26S mutant (1.6 Å) was determined to investigate the cause of the switch in enantiopurity in reactions with substrate (*E*)-**1a**. The data collection and refinement statistics can be found in Table S6 in the Supporting Information. Both structures were virtually identical to previously described monomeric wild-type PETN reductase structures (e.g., PDB ID: 1H50), including the presence of an acetate molecule bound in a similar conformation in the active site (Figure 2A).[21] The structures

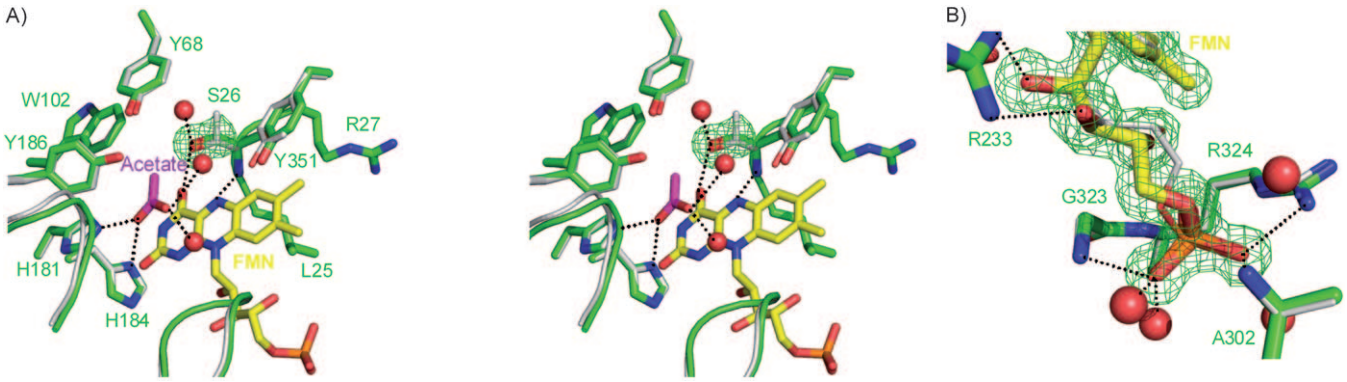

Figure 2. A) Stereo diagram of the X-ray crystal structure of the active site of PETNR mutant T26S superimposed with wild-type enzyme. The T26S structure residues, FMN cofactor and bound acetate ion are shown as atom coloured sticks with green, yellow and magenta carbons, respectively. Residues L25 to R27 are also shown as a green ribbon. The omit $|F_o|-|F_c|$ map of the T26S side chain is contoured at 1 σ (green mesh). B) X-ray crystal structure of the ribityl chain of the FMN of PETNR–His_8 superimposed with wild-type enzyme. The enzyme residues and FMN are shown as atom coloured sticks with green and yellow carbons, respectively. The omit $|F_o|-|F_c|$ map of the FMN molecule is contoured at 1 σ (green mesh). The wild-type structure was obtained from the PDB (ID: 1H50).[21] The wild-type residues are shown as atom coloured lines with grey carbons while waters and interactions are shown as red spheres and black dotted lines, respectively. Residue loops T239–D244 (left) and T273–K279 (right) are shown as green cartoons and grey ribbons, respectively. All figures were generated in PyMOL.[35]

show minor changes in backbone positions of two surface loops near the substrate binding site (T239–D244; T273–K279; Figure 2A) as well as a shift in the orientation and position of the backbone atoms of residue D360. Both structures show a minor "butterfly-bend" in the isoalloxazine ring of the FMN prosthetic group, as seen in the "thermostable-like" OYE member TOYE.[14]

A significant change in the active site of both structures was the orientation of the ribityl chain of FMN starting from atom C3* to the terminal phosphate atoms (Figure 2B and Figure S4 in the Supporting Information). This is similar to the second position of the ribityl chain in the reduced progesterone-bound PETN reductase crystal structure.[23] In spite of these changes, the only difference in the interactions between the ribityl chain and the protein/solvent is the presence of an additional interaction between FMN O1P and R324 N. Residues R324 and A302 are slightly altered in position to enable the wild-type interactions to be maintained in the His_8 structure. Further discussion on the minor differences between the wild-type and His_8-tagged PETN reductase structures can be found in the Supporting Information.

The structure of the active site of PETN reductase T26S mutant revealed only minor changes in the position of residues surrounding the FMN compared to wild type (Figure 2C). The most significant change, albeit minor, was seen in the position of residue Y351, which is known to be involved in substrate/inhibitor binding in OYEs.[22] The omit map $|F_0|-|F_c|$ of residue 26 showed a clear absence of density for the CG2 atom of T26, confirming the presence of the T26S mutation. The mutant retained both its wild-type-like hydrogen bonding interactions between side chain and backbone atoms of S26 and the FMN (S26 OG–FMN O4 and S26 N–FMN N5). Therefore, changes in the activity and stereoselectivity of this mutant are due to more subtle structural changes within the active site.

A sequence alignment of OYE family members shows a high sequence conservation of residue 27 as either threonine or cysteine within the classical and thermophilic-like subclasses, respectively.[14,36] The extensive structural information available for many OYEs shows a highly conserved interaction between the threonine or serine hydroxyl group and the FMN isoalloxazine O4 atom.[22,30] This has been shown to influence the FMN redox potential by stabilising the negative charge of the reduced flavin.[25,37] In addition, the structure of the picric acid-bound wild-type PETN reductase shows that the T26 OG1 atom interacts with the O61 atom (nitro group) of the ligand. Previous modelling studies of PETN reductase with nitro-olefin substrates (*E*)-**19a** to (*E*)-**22a** suggested that multiple binding conformations could be possible, with one position likely to be less favoured due to potential clashes between the substrate Cβ atom and T26 side chain.[26] Therefore, the change in product enantiopreference of product **19b** by the T26S mutant is likely to be due to an increase in binding of the substrate in an alternate conformation made possible by the removal of the Cβ atom of T26. No switch in enantiopreference was seen with the related substrate (*E*)-**21a**, which contains a *p*-chloro substitutent on the aromatic ring; this might restrict the binding of the substrate in the alternate conformation. Therefore, the subtle changes in the active site of PETN reductase caused by the T26S mutation (and W102F) do not effect the binding of all substrates; this highlights the importance of screening multiple libraries of mutants to find suitable biocatalysts with improved functionality against selected substrates.

Conclusions

Our screening procedures were more successful in detecting PETN reductase mutants with significantly improved steady state reactions rather than improvements in enantiopreference and/or *ee* against selected substrates (i.e., "you get what you screen for"). Not all libraries generated improved mutants, suggesting these amino acid positions are not important (at least in isolation) for influencing the reaction rate with these substrates. As expected, our selection criteria were more accurate in finding "hits" with substrates exhibiting large improvement in catalytic rate. To complicate matters, the determination of a true "hit" for improved reaction of poor substrates was problematic because only small changes in an already low activity were detected. Thus, the robotic screen should be used as a first stage in a two-stage screening process and complemented by larger scale tests to determine product yield and enantiopurity. Setting the threshold of criteria higher for determining a "hit" will reduce the overall number of mutants needed to be further characterised, and increase our chance of finding useful mutants.

The advantages of using a steady-state reaction based screening method over biotransformation-based yield and *ee* monitoring include considerably shorter reaction times (10 min vs. 24 h), no downstream product extractions, and the screening of up to three substrates per library extraction. In addition, the purification step not only normalises the enzyme concentration in the reactions, but also dramatically reduces levels of contaminating *E. coli* enzymes that either compete for the substrate or catalyse side reactions on the products.[16] The use of a novel screening facility housed within an anaerobic chamber was essential to eliminate the significant reoxidation rate of NADPH by molecular O_2, especially when poorly reduced oxidising substrates were being tested.

This method enabled us to rapidly screen large numbers of mutants and eliminate significant numbers of library members with compromised activity. This allowed us to dramatically decrease the number of clones required to undergo the more laborious biotransformation reactions. Thus, a hybrid approach has been used incorporating both high-throughput screening by steady state catalytic rates followed by biotransformation reactions with positive screening hits.

Screening methods employing only the detection of reaction rates do not enable us to screen for improvements in *ee* or the maintenance of existing high *ee*. In spite of this, our screen enabled us to detect two mutants (T26S and W102F) with both a switch in product enantiopreference and an increase in *ee*. In addition, the detection of mutants with weak activity against α,β-unsaturated carboxylic acid substrates shows progress in the expansion of substrate scope in PETN reductase. These mutants have given us insight into the impor-

tance of these residues in influencing the relative populations of substrate binding conformations. Recent work by others[16] has showed that more dramatic improvements in biotransformation yields and/or enantioselectivities of mutants tend to be obtained after at least two rounds of iterative saturation mutagenesis; this suggests the importance of cooperative effects of mutants. Given the low numbers of useful mutants detected in our single-site saturation libraries, mutants generated from multiple site-saturated mutagenesis techniques could be rapidly screened in our facility to potentially improve the activity and enantioselectivity of PETN reductase against poorly reduced substrates.

Experimental Section

General: All reagents were of analytical grade. All kinetic measurements were performed within an anaerobic glove box (Belle Technology, Ltd.) under a nitrogen atmosphere (< 5 ppm oxygen). Purified PETN reductase and substrate extinction coefficients used were as described previously.[20,22,29] All medium components were obtained from Formedium. Full gene sequences of all mutants were confirmed by DNA sequencing (Eurofins MWG Operon).

His_8-tag incorporation: A C-terminal His_8-tag was incorporated into an existing high expression PETN reductase construct (pONR1; pBluescript SK^+)[17] by PCR with the overlapping complementary tails method (Figure S1 A in the Supporting Information) based on the QuikChange whole plasmid synthesis protocol (Stratagene). Both the forward and reverse primers contained an 18-base pair (bp) His_6 5′ overhang followed by the native sequence beginning with the stop codon and last PETN reductase residue codon, respectively (CAT CAT CAC CAT CAC CAT TAA TCC CGC TTT GTA CAT TG and ATG GTG ATG GTG ATG ATG CAG TGA AGG GTA GTC GG). The 5′ overhang regions were the only complementary sequences within these primers, with incomplete primer overlap resulting in the production of C-terminal His_8 tags. Constructs were transformed into the *E. coli* strain XL-10 Gold (Stratagene) according to the manufacturer's protocol and incubated on LB medium agar containing ampicillin (100 μg mL^{-1}) for 24 h at 37 °C. Insertion clones were identified by colony pick PCR[19] in which a 302–326 bp C-terminal PCR product was amplified corresponding to the absence and presence of a His_8-tag (CGG GTG CGT ATA CGG CAG AAA AAG C and GCG CAT AAT TTC CTC ATT AAC CAG TCG AAT G for the forward and reverse primers, respectively). Gel electrophoresis in agarose (1.3%) in TAE buffer (40 mM Tris, pH 8.5, containing 1.14 mL glacial acetic acid, 4 mM EDTA) for 1–1.5 h at 100 V was sufficient to visually distinguish between the two small PCR products (Figure S1 B in the Supporting Information). Positive clones were fully sequenced to confirm the presence of the His_8-tag. Sequencing revealed the presence of a silent mutation A921G (DNA sequence) in the original clone, which was propagated throughout the mutants.

Site-directed mutagenesis: Prior to library generation, the mutant T26S (no His_8-tag) was generated by site-directed mutagenesis based on the QuikChange whole plasmid synthesis protocol. PCR reactions were performed by using native pONR1[17] as the template and the oligonucleotides GGC CCC ACT TAG CCG TCT GCG CA and TGC GCA GAC GGC TAA GTG GGG CC. Constructs were transformed into the *E. coli* strain JM109 (Promega) according to the manufacturer's protocol and incubated on LB agar containing ampicillin (100 μgmL^{-1}) for 24 h at 37 °C. Positive clones were fully sequenced to confirm the presence of the T26S mutation.

Generation of site-saturated single position libraries of PETN reductase-His_8: Amino acid randomisation was performed by using protocols based on the CASTing method of mutagenesis.[38] Single site-saturated libraries were generated at selected amino acid positions (T26, Y68, W102, H181, H184, Y186, Q241 and Y351) by PCR with NNK degenerate oligonucleotides (T26X: GTT TAT GGC CCC ACT TNN KCG TCT GCG CAG CAT CG, CGA TGC TGC GCA GAC GMN NAA GTG GGG CCA TAA AC; Y68X: GCT CAG GCA AAA GGC NNK GCC GGT GCA CCG GG, CCC GGT GCA CCG GCM NNG CCT TTT GCC TGA GC; W102X: CGT ATT GCG GTT CAG CTG NNK CAC ACC GGT CGT ATC, GAT ACG ACC GGT GTG MNN CAG CTG AAC CGC AAT ACG; H181X: CGA CCT GGT TGA GCT TNN KTC TGC GCA CGG TTA CC, GGT AAC CGT GCG CAG AMN NAA GCT CAA CCA GGT CG; H184X: GTT GAG CTT CAC TCT GCG NNK GGT TAC CTG CTG CAT CAG, CTG ATG CAG CAG GTA ACC MNN CGC AGA GTG AAG CTC AAC; Y186X: CAC TCT GCG CAC GGT NNK CTG CTG CAT CAG TTC CTG, CAG GAA CTG ATG CAG CAG MNN ACC GTG CGC AGA GTG; Q241W: CCC CGA TCG GTA CTT TCN NKA ACG TCG ACA ACG GTC, GAC CGT TGT CGA CGT TMN NGA AAG TAC CGA TCG GGG; Y351X: GTC CTG AAA GCT TCN NKG GCG GCG GCG CGG, CCG CGC CGC CGC CMN NGA AGC TTT CAG GAC). Following template removal by selective restriction digestion (DpnI), PCR products (50 ng) were transformed into the *E. coli* strain JM109 (Promega) according to the manufacturer's protocol. Each library of transformants were grown on three plates of LB agar containing ampicillin (100 μg mL^{-1}) for 24 h at 37 °C to a density of 150–300 colonies per plate. To generate a non-mutation control library, the wild-type enzyme–His_8 construct was transformed into the same *E. coli* strain and processed as above.

Anaerobic robotic library screening protocols: All robotic screening procedures were carried out by using a custom-designed Microlab Star platform (Hamilton Robotics; Figure S5 in the Supporting Information) located within an anaerobic glove box under a nitrogen atmosphere (< 5 ppm oxygen; Belle Technology) to avoid false positive enzyme activity detection due to unproductive flavin reoxidation by oxygen.

1) Colony picking: Automated colony picking was used to pick 96 colonies per agar plate. These were used to inoculate terrific broth medium (TB; 96 × 1 mL) containing ampicillin (200 μg mL^{-1}) in 2.2 mL 96-deep-well blocks. The cultures were sealed with a sterile gas-permeable membrane (StarLab) and incubated aerobically for 16 h at 37 °C in a plate incubator (Titramax 1000, Heidolph) at 1050 rpm. Glycerol stocks of each library were produced by combining the culture (50 μL) with a cryoprotectant buffer (80%, *v*/*v*) phosphate buffered saline[39] containing glycerol (20%, *v*/*v*; 50 μL) within 96-well PCR plates and stored at −80 °C.

2) PETN reductase library culture generation: Each library of clones was grown in TB autoinduction medium (TBAIM; 1.0 mL) containing ampicillin (200 μg mL^{-1}) in 96-deep-well blocks as before for 24 h, by using the glycerol stocks as the inoculums. The cultures were harvested by centrifugation for 20 min at 1109 *g* in an Allegra X-22R bench top centrifuge (Beckman Coulter) after replacement of the gas-permeable seal for an aluminium foil lid (Beckman Coulter). The pellets were retained within the 96-well block and stored at −20 °C.

3) Robotic protein purification: High-throughput PETN reductase protein extraction and microscale purification was achieved robotically in a 96-well format, by using Ni-magnetic agarose beads (Novagen) as an affinity resin specific for the His-tag. Cell pellets were completely lysed by the addition of buffer A (50 mM KH_2PO_4/K_2HPO_4, pH 7.9, 200 μg mL^{-1} lysozyme, 15 UmL^{-1} benzonase (Nova-

gen); 200 μL), followed by ten rapid mixing cycles. The lysates were agitated for 5 min followed by the addition of buffer B (1.5 M NaCl, 0.2 M imidazole, pH 7.9, 1 mM FMN; 50 μL) to reduce subsequent unspecific protein binding to the affinity resin and to ensure maximal flavination of PETN reductase. A slurry of Ni-magnetic agarose beads (1% beads in 50 mM KH_2PO_4/K_2HPO_4, pH 7.9, 0.3 M NaCl, 5 mM imidazole and 40% (*w/v*) sorbitol; 50 μL) was added to the lysates followed by agitation for 3 min to maximise PETN reductase binding. Sorbitol was added to the magnetic beads resuspension buffer to increase the viscosity and ensure more even dispension of beads across the plate. Automated lysate removal (and subsequent wash/elution buffer removal) was achieved after affinity resin immobilisation by using a 96-well magnet (Qiagen). The resin was washed three times by resuspension in buffer C (50 mM KH_2PO_4/K_2HPO_4, pH 7.9, 0.3 M NaCl, 250 mM imidazole; 700 μL then 2×200 μL). PETN reductase was eluted in buffer D (50 mM KH_2PO_4/K_2HPO_4, pH 7.9, 0.3 M NaCl, 250 mM imidazole; 120 μL) into 96-well microtiter plates (Greiner) containing buffer E (50 mM KH_2PO_4/K_2HPO_4, pH 7.0; 180 μL).

4) Robotic library activity screening: Automated anaerobic steady-state kinetics assays of library eluants were performed in 96-well UV transparent plates (Greiner) by monitoring the consumption of NADPH in the presence of an oxidising alkene substrate.[20] Reactions (0.3 mL) were performed in buffer (50 mM KH_2PO_4/K_2HPO_4, pH 7.0) containing NADPH (100 μM) and alkene (1 mM added as concentrated stocks in ethanol), and started by the addition of PETN reductase eluant (50–150 μL). The reactions were continuously monitored at 340 nm for 10 min at 25 °C in a Biotek Synergy HT microtiter plate reader. Rates of each library member with each substrate were compared to the average activity from 96 wild-type clones. In addition, potential "hits" were identified by calculating the relative *Z* scores for each mutant [Eq. (1)]:[26]

$$Z_i = (x_i - X)/S_x \quad (1)$$

where X is the mean of all the sample values x_i (no controls) of the library, and S is the standard deviation of these values.

Medium-scale protein production and purification: PETN reductase–His_8 wild-type and mutant cultures (1–6 L) were grown in TBAIM containing ampicillin (100 μg mL^{-1}) for 24 h at 37 °C. Cells were harvested by centrifugation at 6000 *g* for 30 min at 5 °C (Avanti J-26 XP; Beckman Coulter). Cell pellets were resuspended in lysis buffer (50 mM KH_2PO_4/K_2HPO_4, pH 8.0, containing the EDTA-free complete protease inhibitor cocktail (Roche), 0.1 mg mL^{-1} DNase I, 1 mg mL^{-1} lysozyme and excess free FMN) and stirred for 30 min at 4 °C. Cells were disrupted by sonication (Sonics Vibra Cell) followed by extract clarification by centrifugation for 20 min at 26600 *g*.

PETN reductase–His_8 was purified by binding to a 50 mL Ni-NTA column (Qiagen), pre-equilibrated in buffer A (50 mM KH_2PO_4/K_2HPO_4, pH 8.0, 0.3 M NaCl, 20 mM imidazole). The column was washed with 5×column volumes of buffer B (50 mM KH_2PO_4/K_2HPO_4, pH 8.0, 0.3 M NaCl, 40 mM imidazole) followed by elution in a step to buffer C (50 mM KH_2PO_4/K_2HPO_4, pH 8.0, 0.3 M NaCl, 250 mM imidazole). Purity was assessed by SDS-PAGE and the concentration determined by using the extinction coefficient method.[20,22]

Crystallogenesis and data collection: Crystals of oxidised wild-type PETN reductase–His_8 and the T26S (no tag) were grown by using the sitting-drop method in sodium cacodylate, pH 6.2, (100 mM) containing sodium acetate (0.1 M), isopropanol (16–18%) and poly(ethylene glycol) 3000 (18–22%) for 3 days at 20 °C. The crystals were flash frozen in liquid nitrogen in the absence of additional cryoprotectant. A full PETN reductase–His_8 (1.4 Å) X-ray diffraction data set were collected from a single crystal at the European Synchrotron Radiation Facility (Grenoble, France) on Station ID 14.4 (wavelength 1.07 Å; 100 K) by using an ADSC CCD detector. A full T26S PETN reductase (1.5 Å) X-ray diffraction data set was collected in-house from a single crystal by using a Rigaku Micromax007 generator (wavelength 0.97 Å; 100 K) with an R-Axis IV^{++} detector.

Structure determination and refinement: Both data sets were processed and scaled by using the programs MOSFLM[40] and Scala.[41] The structures were solved by molecular replacement by using the coordinates for the acetate-bound PETN reductase structure (PDB ID: 1H50).[21] Model rebuilding and water addition was performed automatically by using REFMAC combined with ARP/warp.[42] Positional and anisotropic B-factor refinement was performed by using REFMAC5,[41] (hydrogen atoms included in the refinement) with alternate rounds of manual rebuilding of the model in COOT.[43] The final models were refined to 1.40, 1.50 and 1.6 Å resolution giving final R_{factor}/R_{free} of 12.6/15.6 and 14.7/17.0 for PETN reductase–His_8 and T26S mutant, respectively. The atomic coordinates and structure factors for PETN reductase-His8 (ID: 3P62) and for the T26S mutant (ID: 3P67) have been deposited in the Protein Data Bank, Research Collaboratory for Structural Bioinformatics, Rutgers University, New Brunswick, NJ (http://www.rcsb.org/)

Chemistry: NMR spectra were recorded on 400 or 500 MHz spectrometers and referenced to the solvent, unless stated otherwise. The chemical shifts are reported in ppm and coupling constants (*J*) are given in hertz (Hz). Melting points were determined by using electrothermal capillary apparatus and are uncorrected. IR spectra were recorded neat on NaCl plates. HPLC analysis was performed by using an instrument equipped with a UV detector. UV/Vis data were recorded with a diode array spectrophotometer. The reaction progress was monitored by GC or TLC on standard silica gel plates. All chemicals were obtained from commercial sources and the solvents were of analytical grade. Substrates **1a**–**15a**, (5*R*)-**16a** and **17a** and dihydro products **1**–**9b**, **12b**–**15b** and **17b** were obtained from commercial suppliers (Aldrich and Alfa Aesar). (+)-Dihydrocarvone was obtained from a commercial supplier as a mixture of two isomers (2*R*,5*R*)-**16b** and (2*R*,5*S*)-**16b** in a 77:20 ratio (>99% *ee*). Nitroalkenes (*E*)-**19a** and (*E*)-**21a** were synthesised as described previously.[22,29] Racemic nitroalkane **21b** were obtained in 80–85% yields by silica gel-assisted reduction of their respective nitroalkenes with $NaBH_4$, as described in the literature.[44] Model optically active nitroalkane (*R*)-**21b** was synthesized as described before.[45] The substrates **2a**, **5a**, **18a** and products **2b**, **5b**, (2*R*,5*R*)-**16b** and (*R*)-**17b**–(*R*)-**18b**, were synthesised as described previously.[20,22,29] The nitroalkenes (*E*)-**19a** to (*E*)-**22a** and their respective alkene products (*R*/*S*)-**19b** to (*R*/*S*)-**22b** were synthesised as described previously.[20,45] The remaining compounds were synthesized as follows:

1) 2-Methyl-3-phenyl-propan-1-ol (*rac*) (***4c***)*:* This was synthesised from a mixture of (*E*)-2-methyl-3-phenyl-prop-2-en-1-ol (10.0 mmol) and Pd-C (10%, 0.10 g) in ethyl acetate (150 mL) stirred under H_2 (g) for 24 h. The catalyst was removed by filtration through a pad of Celite and the solvent was removed in vacuo. The crude product was purified by flash column chromatography (hexane/ethyl acetate, 9:1, 4:1) to give 2-methyl-3-phenylpropanol (1.43 g, 95.3%). ^{1}H NMR (400 MHz; $CDCl_3$): $\delta = 0.92$ (d, $J = 6.8$ Hz, 3H; CH_3). 1.28 (br s, 1H; OH), 1.90–2.00 (m, C1H; H), 2.43 (dd, $J = 13.4$, 8.0 Hz, 1H; CH_AH_B), 2.76 (dd, $J = 13.4$, 6.3 Hz, 1H; CH_AH_B), 3.48 (dd, $J = 10.5$,

6.2 Hz, 1H; CH_AH_B-OH), 3.54 (dd, J=10.7, 5.9 Hz, 1H; CH_AH_B-OH), 7.15–7.32 (m, 5H; Ph); ^{13}C NMR (101 MHz; $CDCl_3$): δ=140.7 (s, Cq), 129.27 (s, 2CH), 128.4 (s, 2CH), 126.0 (s, CH), 67.8 (s, CH_2), 39.8 (s, CH_2), 37.92 (s, CH), 16.59 (s, CH_3).

*2) (rac)-2-Phenylpropan-1-al oxime (**19c**)*: This was synthesised from its respective aldehyde (10.0 mmol) by refluxing for 4 h in ethanol (60 mL), hydroxylamine hydrochloride (19.0 mmol) and sodium acetate (dry). The reaction was poured into water and extracted with DCM, dried ($MgSO_4$ powder) and evaporated, in vacuo. The residue was purified by chromatography to yield **19c** as an oil, which was a mixture of two isomers *E*/*Z* 2.54:1 for both compounds. ^{1}H NMR (400 MHz, $CDCl_3$): δ=1.44 (d, J=6.8 Hz, CH_{3min}), 1.46 (d, J=6.8 Hz, CH_{3maj}), 3.68 (pentet, J=6.8 Hz, CH_{maj}), 4.45 (pentet, J=7.2 Hz, CH_{min}), 6.83 (d, J=7.6 Hz, N=CH_{min}), 7.21–7.37 (m, 5H), 7.53 (d, J=6.0 Hz, N=CH_{maj}); ^{13}C NMR (100 MHz, $CDCl_3$): δ=18.3, 18.8, 34.9, 40.4, 126.7, 126.9, 127.2, 127.4, 128.7, 128.8, 141.9, 154.9.

Analytical procedures: GC analysis of conversion and yields was performed on a 30 m DB-Wax (0.32 mm, 0.25 mm) column as described previously.[20,22,29] Yields of compounds (*rac*)-**4c** and oximes (*rac*)-**19c** and (*rac*)-**21c** were determined by GC analysis as described previously for their respective alkene substrate derivatives.[20,22,29] HPLC analysis of conversion, yields and enantiomeric excess of **4a** and (*R*/*S*)-**4b** was performed on a Chiracel OJ column (hexane/*i*PrOH, 99:1 at 18 °C, flow 1 mL min^{-1}, t_R: (*R*)- and (*S*)-dihydro-methylcinnamaldehyde 11.5 and 14.6 min, respectively). The detector wavelength was 195 nm. Determination of the enantiomeric excess and absolute configuration of all other compounds were performed as described previously.[20,22,29,31]

Biotransformations of alkenes by PETN reductase: Standard reactions for screening library mutants (1.0 mL) were performed in buffer (50 mM KH_2PO_4/K_2HPO_4, pH 7.0) containing alkene (5 mM; added as a concentrated stock in ethanol to a 5% final concentration), NADPH (6 mM) and PETN reductase (2 μM). The reactions were shaken at 37 °C at 130 rpm for 24 h followed by reaction termination by extraction with ethyl acetate (0.9 mL) containing an internal standard (0.5% limonene), and dried by using $MgSO_4$. The extracts were analysed by GC or HPLC to determine the %yield, %conversion, and enantiomeric excess as described above.[20,22,29] Comparative biotransformation reactions between wild-type and T26S enzyme were carried out as above, except for the use of a $NADP^+$/glucose-6-phosphate dehydrogenase or $NADP^+$/glucose dehydrogenase cofactor regeneration system[20,22] in the place of NADPH with a reaction temperature of 30 °C. Biphasic reactions were carried out as described previously.[20,22]

Steady-state kinetic analysis: The enzymes were deoxygenated by passage through a BioRad 10DG column equilibrated in anaerobic reaction buffer. Steady state analyses were performed on a Cary UV-50 Bio UV/Vis scanning spectrophotometer by using a quartz cuvette (1 mL; Hellma) with a 1 cm path length. Reactions (1 mL) were performed in buffer (50 mM KH_2PO_4/K_2HPO_4, pH 7.0) containing NADPH (0.1 mM), PETN reductase (0–5 μM) and oxidative substrate (1 mM added as concentrated stocks in ethanol to a final concentration of 5%, *v*/*v*). The reactions were followed continuously by monitoring NADPH oxidation at 340 nm for 1 min at 25 °C. Reactions with oxidizing substrates that absorb at 340 nm were monitored at 365 nm. The concentration of enzyme, NADPH and substrates within the reactions were determined by the extinction coefficient method by using values determined previously.[20]

Fast reaction kinetics: Reductive and oxidative half reaction kinetic experiments with PETN wild-type and His_8 reductase were performed anaerobically by using an Applied Photophysics SX.18MV-R stopped-flow spectrophotometer. The transients were analysed by using nonlinear least squares regression analysis on an Acorn Risc PC microcomputer with Spectrakinetics software (Applied Photophysics). The reductive half reactions (1.0 mL) were performed in buffer (50 mM KH_2PO_4/K_2HPO_4, pH 7.0) containing NADPH (0.05–1 mM) and PETN reductase (10 μM). The oxidative half reactions (1.0 mL) were performed in buffer (50 mM KH_2PO_4/K_2HPO_4, pH 7.0) containing dithionite-reduced PETN reductase (10 μM) and 2-cyclohexan-1-one (2.5–50 mM). Absorption change of flavin reduction/reoxidation was monitored continuously at 464 nm at 25 °C for 1 s. The concentrations of substrates were always at least tenfold greater than the enzyme concentration, ensuring pseudo-first order conditions. The data points are the average of at least three transients. The transients were fitted to a single exponential plot from which observed rates were determined by using the rapid equilibrium formalism of Strickland et al[46] [Eq. (2)] for the following kinetic scheme [Eq. (3)].

$$k_{ox} = k_3[S]/(K_d + [S]) \quad (2)$$

$$A + B \overset{k_1}{\leftrightarrow} C \xrightarrow{k_3} D \quad (3)$$

Acknowledgements

We thank Victoria Hare for assistance in the generation and crystallography of PETN reductase T26S mutant. M.H. was supported by a UK Biotechnology and Biological Sciences Research Council (BBSRC) studentship. This work was funded by the BBSRC. N.S.S. is a BBSRC Professorial Research Fellow and a Royal Society Wolfson Merit Award holder.

Keywords: asymmetric bioreduction · biocatalysis · directed evolution · enantioselectivity · robotic library screening

[1] N. J. Turner, *Trends Biotechnol.* **2003**, *21*, 474–478.
[2] R. R. Chirumamilla, R. Muralidhar, R. Marchant, P. Nigam, *Mol. Cell. Biochem.* **2001**, *224*, 159–168.
[3] S. Panke, M. Held, M. Wubbolts, *Curr. Opin. Biotechnol.* **2004**, *15*, 272–279.
[4] M. T. Reetz, D. Kahakeaw, J. Sanchis, *Mol. Biosyst.* **2009**, *5*, 115–122.
[5] S. Luetz, L. Giver, J. Lalonde, *Biotechnol. Bioeng.* **2008**, *101*, 647–653.
[6] M. T. Reetz, *Angew. Chem.* **2010**, *122*, DOI: 10.1002/ange.201000826; *Angew. Chem. Int. Ed.* **2010**, *49*, DOI: 10.1002/anie.201000826; M. T. Reetz, M. Bocola, L. W. Wang, J. Sanchis, A. Cronin, M. Arand, J. Zou, A. Archelas, A. L. Bottalla, A. Naworyta, S. L. Mowbray, *J. Am. Chem. Soc.* **2009**, *131*, 7334–7343.
[7] N. M. Antikainen, S. F. Martin, *Bioorg. Med. Chem.* **2005**, *13*, 2701–2716.
[8] R. Stuermer, B. Hauer, M. Hall, K. Faber, *Curr. Opin. Chem. Biol.* **2007**, *11*, 203–213.
[9] M. Hall, C. Stueckler, W. Kroutil, P. Macheroux, K. Faber, *Angew. Chem.* **2007**, *119*, 4008–4011; *Angew. Chem. Int. Ed.* **2007**, *46*, 3934–3937.
[10] J. F. Chaparro-Riggers, T. A. Rogers, E. Vazquez-Figueroa, K. M. Polizzi, A. S. Bommarius, *Adv. Synth. Catal.* **2007**, *349*, 1521–1531; M. Hall, C. Stueckler, H. Ehammer, E. Pointner, G. Oberdorfer, K. Gruber, B. Hauer, R. Stuermer, W. Kroutil, P. Macheroux, K. Faber, *Adv. Synth. Catal.* **2008**, *350*, 411–418; M. Hall, C. Stueckler, B. Hauer, R. Stuermer, T. Friedrich, M. Breuer, W. Kroutil, K. Faber, *Eur. J. Org. Chem.* **2008**, 1511–1516; M. Hall, C. Stueckler, B. Hauer, R. Stuermer, W. Kroutil, P. Macheroux, K. Faber in *Biotrans—8th International Symposium on Biocatalysis and Biotransformations*, Oviedo, Spain, **2007**; C. Stueckler, M. Hall, H. Ehammer, E. Pointner, W. Kroutil, P. Macheroux, K. Faber, *Org. Lett.* **2007**, *9*, 5409–5411; M. A. Swiderska, J. D. Stewart, *Org. Lett.* **2006**, *8*, 6131–6133; M. A. Swiderska, J. D. Stewart, *J. Mol. Catal. B* **2006**, *42*, 52–54.

[11] O. Warburg, W. Christian, *Naturwissenschaften* **1932**, *20*, 688.
[12] P. R. Binks, C. E. French, S. Nicklin, N. C. Bruce, *Appl. Environ. Microbiol.* **1996**, *62*, 1214 – 1219.
[13] T. B. Fitzpatrick, N. Amrhein, P. Macheroux, *J. Biol. Chem.* **2003**, *278*, 19891 – 19897.
[14] B. V. Adalbjörnsson, H. S. Toogood, A. Fryszkowska, C. R. Pudney, T. A. Jowitt, D. Leys, N. S. Scrutton, *ChemBioChem* **2010**, *11*, 197 – 207.
[15] S. K. Padhi, D. J. Bougioukou, J. D. Stewart, *J. Am. Chem. Soc.* **2009**, *131*, 3271 – 3280.
[16] D. J. Bougioukou, S. Kille, A. Taglieber, M. T. Reetz, *Adv. Synth. Catal.* **2009**, *351*, 3287 – 3305.
[17] C. E. French, S. Nicklin, N. C. Bruce, *J. Bacteriol.* **1996**, *178*, 6623 – 6627.
[18] M. K. Trower, *Methods Mol. Biol.* **1996**, *58*, 329 – 333.
[19] T. B. Fitzpatrick, S. Auweter, K. Kitzing, T. Clausen, N. Amrhein, P. Macheroux, *Protein Expr. Purif.* **2004**, *36*, 280 – 291.
[20] A. Fryszkowska, H. S. Toogood, M. Sakuma, J. M. Gardiner, G. M. Stephens, N. S. Scrutton, *Adv. Synth. Catal.* **2009**, *351*, 2976 – 2990.
[21] T. M. Barna, H. Khan, N. C. Bruce, I. Barsukov, N. S. Scrutton, P. C. Moody, *J. Mol. Biol.* **2001**, *310*, 433 – 447.
[22] K. M. Fox, P. A. Karplus, *Structure* **1994**, *2*, 1089 – 1105.
[23] H. Khan, T. Barna, N. C. Bruce, A. W. Munro, D. Leys, N. S. Scrutton, *FEBS J.* **2005**, *272*, 4660 – 4671.
[24] H. Khan, R. J. Harris, T. Barna, D. H. Craig, N. C. Bruce, A. W. Munro, P. C. Moody, N. S. Scrutton, *J. Biol. Chem.* **2002**, *277*, 21906 – 21912.
[25] H. L. Messiha, N. C. Bruce, B. M. Sattelle, M. J. Sutcliffe, A. W. Munro, N. S. Scrutton, *J. Biol. Chem.* **2005**, *280*, 27103 – 27110.
[26] H. S. Toogood, A. Fryszkowska, V. Hare, K. Fisher, A. Roujeinikova, D. Leys, J. M. Gardiner, G. M. Stephens, N. S. Scrutton, *Adv. Synth. Catal.* **2008**, *350*, 2789 – 2803.
[27] C. Brideau, B. Gunter, B. Pikounis, A. Liaw, *J. Biomol. Screening* **2003**, *8*, 634 – 647.
[28] C. Stueckler, N. J. Mueller, C. K. Winkler, S. M. Glueck, K. Gruber, G. Steinkellner, K. Faber, *Dalton Trans.* **2010**, *39*, 8472 – 8476.
[29] P. Galletti, E. Emer, G. Gucciardo, A. Quintavalla, M. Pori, D. Giacomini, *Org. Biomol. Chem.* **2010**, *8*, 4117 – 4123.
[30] H. Khan, T. Barna, R. J. Harris, N. C. Bruce, I. Barsukov, A. W. Munro, P. C. Moody, N. S. Scrutton, *J. Biol. Chem.* **2004**, *279*, 30563 – 30572.
[31] N. K. Scheffler, S. W. Miller, A. K. Carroll, C. Anderson, R. E. Davis, S. S. Ghosh, B. W. Gibson, *Mitochondrion* **2001**, *1*, 161 – 179.
[32] K. Durchschein, B. Ferreira-da Silva, S. Wallner, P. Macheroux, W. Kroutil, S. M. Glueck, K. Faber, *Green Chem.* **2010**, *12*, 616 – 619.
[33] H. Ohta, N. Kobayashi, K. Ozaki, *J. Org. Chem.* **1989**, *54*, 1802 – 1804.
[34] K. Kitzing, T. B. Fitzpatrick, C. Wilken, J. Sawa, G. P. Bourenkov, P. Macheroux, T. Clausen, *J. Biol. Chem.* **2005**, *280*, 27904 – 27913.
[35] W. L. DeLano, *The PyMOL User's Manual*, DeLano Scientific, Palo Alto, CA, USA, **2002**.
[36] H. S. Toogood, J. M. Gardiner, N. S. Scrutton, *ChemCatChem* **2010**, *2*, 892 – 914.
[37] D. Xu, R. M. Kohli, V. Massey, *Proc. Natl. Acad. Sci. USA* **1999**, *96*, 3556 – 3561.
[38] C. M. Clouthier, M. M. Kayser, M. T. Reetz, *J. Org. Chem.* **2006**, *71*, 8431 – 8437; M. T. Reetz, L. W. Wang, M. Bocola, *Angew. Chem.* **2006**, *118*, 1258 – 1263; *Angew. Chem. Int. Ed.* **2006**, *45*, 1236 – 1241.
[39] J. Sambrook, E. F. Fritsch, T. Maniatis, *Molecular Cloning: A Laboratory Manual, Vol. 3*, 2nd ed., Cold Spring Harbor Laboratory Press, New York, **1989**, appendix B.12.
[40] A. G. W. Leslie in *Joint CCP4 & ESRF-EACBM Newsletter on Protein Crystallography, Vol. 26*, Serc Laboratory, Daresbury, Warrington, UK, **1992**.
[41] Collaborative Computational Project Number 4, *Acta Crystallogr. Sect. D Biol. Crystallogr.* **1994**, *50*, 760 – 763.
[42] A. Perrakis, R. Morris, V. S. Lamzin, *Nat. Struct. Biol.* **1999**, *6*, 458 – 463.
[43] P. Emsley, K. Cowtan, *Acta Crystallogr. Sect. D Biol. Crystallogr.* **2004**, *60*, 2126 – 2132.
[44] A. K. Sinhababu, R. T. Borchardt, *Tetrahedron Lett.* **1983**, *24*, 227 – 230.
[45] A. Fryszkowska, K. Fisher, J. M. Gardiner, G. M. Stephens, *J. Org. Chem.* **2008**, *73*, 4295 – 4298.
[46] S. Strickland, G. Palmer, V. Massey, *J. Biol. Chem.* **1975**, *250*, 4048 – 4052.

Received: September 3, 2010
Published online on November 9, 2010

